ISSN 0965-5425, Computational Mathematics and Mathematical Physics, 2019, Vol. 59, No. 6, pp. 1006–1014. © Pleiades Publishing, Ltd., 2019.
Russian Text © The Author(s), 2019, published in Zhurnal Vychislitel'noi Matematiki i Matematicheskoi Fiziki, 2019, Vol. 59, No. 6, pp. 1037–1046.

The Use of Wall Functions for Simulating the Turbulent Thermal Boundary Layer

V. R. Efremov[a,*], V. V. Kurulin[b,], A. S. Kozelkov[b,c,***], A. A. Kurkin[c,****], and D. A. Utkin[b,*****]**

[a] *Instrument Design Bureau, Tula, 300001 Russia*

[b] *Russian Federal Nuclear Center—All-Russia Institute of Experimental Physics, Sarov, Nizhegorodskaya oblast, 607189 Russia*

[c] *Nizhny Novgorod State Technical University, Nizhny Novgorod, 603950 Russia*

**e-mail: valentin_e@mail.ru*

***e-mail: kurulin@mail.ru*

****e-mail: askozelkov@mail.ru*

*****e-mail: aakurkin@gmail.com*

******e-mail: dimitryavich@yandex.ru*

Received June 30, 2018; revised September 14, 2018; accepted February 8, 2019

Abstract—An important problem in the numerical simulation of turbulent heat exchange in fluids is accurate prediction of hydrodynamic characteristics of the flow in the boundary layer, which requires a fine grid near rigid surfaces. In applications, it is not always possible to have a fine grid and the use of a coarser grid results in significant loss of accuracy. A well-known approach to improving the accuracy of the numerical simulation of the boundary layer is the use of universal wall functions for computing the friction and thermal flux. In this paper, we consider the known wall functions for computing the thermal flux. The accuracy of these functions in problems of turbulent nonisothermal flow of fluid is studied. These are the flow in a plane channel, Couette flow, and flow along a heated plate. Each of these problems is solved on grids with various near wall resolutions. The results of solving these problems provide a basis for estimating the accuracy of the wall functions used for solving them. It is shown that the wall functions considered in this study yield nonmonotonic convergence of the results as the grid is refined.

Keywords: numerical simulation, turbulence, boundary layer, turbulent heat exchange, wall function

DOI: 10.1134/S0965542519060058

INTRODUCTION

A large part of practically important flows of fluids is turbulent and contains portions of the boundary layer near a rigid surface. The boundary layer has a complex structure, and it is characterized by high gradients of the longitudinal velocity and temperature. The gradient of velocity in the boundary layer directly determines the friction force and, therefore, the total hydrodynamical drag [1]. In turn, the gradient of temperature determines the thermal flux transferred from the fluid to the rigid body. For this reason, the accuracy of numerical simulation of most problems directly depends on the accuracy of the boundary layer.

Methods of numerical simulation of the boundary layer are determined by the approaches used to simulate turbulence. For example, in the case of direct numerical simulation, eddies of all linear scales, including Kolmogorov's scale, must be reproduced in the boundary layer (see [2]). This requires the use of detailed grid models, which requires prohibitively high computational resources [3–5]. Presently, the RANS models of turbulence [6, 7] are the best available models for simulating turbulent flows of fluids. In the RANS model, the instantaneous fields of basic quantities are replaced by averaged fields. This makes it possible to significantly reduce the number of grid cells in the boundary layer. However, the gradients of the averaged fields of velocity and temperature in the direction orthogonal to the wall remain high in the boundary layer, and they require a fine grid in this domain.

The quality of grid resolution is determined by the distance from the wall to the first grid node, which must be deep in the laminar sublayer to provide good results; this corresponds to the value of the dimen-

sionless parameter $y^+ < 1$ (see [1]). In many problems, the construction of the computation grid with such a near-wall resolution runs into difficulties because the flow velocity can change by several orders of magnitude near the same rigid surface, which implies a similar variation of the dimensionless parameter y^+. In such problems, the construction of a computation grid satisfying the condition that the first near wall layer is within the laminar sublayer along the entire rigid surface ($y^+ < 1$), results in the increase of the number of grid cells and emergence of zones with an excessive number of cells that do not improve the results but consume computational resources. On the other hand, the failure to satisfy this condition even for small portions of the rigid surface yields poor results because already for $y^+ > 10$ the direct method of computing the friction force on the wall gives a significant error [8, 9].

A way out is to use universal wall functions that make it possible to accurately predict the friction coefficient and velocity derivative on the rigid wall in a wide range of values of the parameter y^+. The method of wall functions became popular after the publication of the paper by Launder and Spalding [8] and has since become an indispensible tool for working with RANS turbulence models. This method is based on initializing the boundary conditions for the equation of conservation of momentum and energy at a certain distance from the wall outside the laminar sublayer rather than on the wall itself. The boundary conditions are moved into the region of turbulent near wall layer, which reduces the number of grid cells in the normal direction to the wall. The basic assumptions of the method of wall functions are the universality of the logarithmic velocity and temperature profile in the near wall region and the constancy of the shear stress, thermal flux, and turbulent energy [10]. For this reason, wall functions for approximating the longitudinal velocity profile and thermal wall functions are distinguished. The application of wall functions makes it possible to simulate near wall phenomena that are characteristic for turbulence. However, this method requires further elaboration to enable it to take into account low Reynolds elements of the turbulence model (see [8]).

The further elaboration of the method of wall functions reduces to expanding the range of their application due to improving the accuracy in the laminar sublayer. For example, in [11] a wall thermal function is obtained that automatically resolves the laminar sublayer and the logarithmic subregion of the boundary layer. It is shown that the results obtained using this function are in good agreement with experimental data for the Prandtl numbers $\mathrm{Pr} \gg 1$. However, no comparison of the results obtained on grids with different resolutions is given in [11].

In [12], an approximation that includes three types of wall functions for resolving the boundary layer for the laminar, buffer, and logarithmic sublayers is proposed. These functions make it possible to compute the thermal flux at the Prandtl numbers $y^+\mathrm{Pr} < 1$, $y^+\mathrm{Pr} = 1 - 11.7$, and $y^+\mathrm{Pr} > 11.7$, respectively. The proposed wall functions make it possible to simulate the boundary layer in a wide range of Prandtl numbers; however, these functions must be improved for solving special problems; this improvement is to calibrate formulas relative to the reference solution results.

In [13], versions of the temperature and velocity wall functions for materials with different values of the Prandtl number are derived from the differential equations of conservation of energy and momentum, respectively. For air ($\mathrm{Pr} \sim 0.7$), the analytical dependence thus obtained is in good agreement with experimental data; however, the analytical dependence for water ($\mathrm{Pr} \sim 5.9$) cannot provide good agreement with experimental data because the thickness of the thermal boundary layer becomes less than the thickness of the dynamic layer; this requires the values of the eddy viscosity and the turbulent Prandtl number for fluids with $\mathrm{Pr} \gg 1$ at small y^+ to be determined more accurately.

In [10], the influence of such factors as flows on impermeable surfaces with a nonzero pressure gradient, flows on permeable surfaces with a zero pressure gradient, and free convection on impermeable and permeable surfaces, which complicate the flow, on wall functions is analyzed. It is justified that there are no universal wall functions, but they should be chosen depending on the class of flows under examination.

The recent paper [11], which concerns the influence of the near wall step on the flow pattern, is devoted to the computation of separated flows of the incompressible viscous fluid within the model of shear stress transfer (MSST). The authors considered the flow around a disk–cylinder arrangement with the ultralow profile drag and gave a detailed analysis of the fields of applicability of wall functions for some turbulence models; they also distinguished the cases in which the application of wall functions is appropriate.

Such a diversity of wall functions is explained by attempts to reduce errors when these functions are applied to various classes of problems. In this paper, we study the accuracy of wall functions of the existing thermal wall functions as applied to forced convection with a thermal boundary layer. We consider the following wall functions: the one defined in [12], which uses the interpolation coefficient for the smooth switching between the expression for the logarithmic and turbulent subregions; the function defined

in [14], which was obtained for computation with Prandtl numbers for gases; and the function defined in [13], which uses a special expression for the buffer subregion of the thermal boundary layer. As benchmark problems, we consider the flow in a plane channel with heated walls and volumetric heat release [15], Couette flow [1], and flow around a heated plate [17]. Each of these problems is solved on grids with different near wall resolution. On the basis of the computational results, we estimate the accuracy of each wall function. We also discuss the monotonicity of the results depending on the grid refinement in the vicinity of the boundary layer.

1. SIMULATION OF THE THERMAL BOUNDARY LAYER

The definition of wall functions is reduced to establishing a relationship between the parameters T^+ and y^+ using empirical formulas. Here T^+ is the temperature on the wall made nondimensional using the wall temperature T_w and the temperature in the first node T_i, density ρ, the specific heat capacity C_P, dynamic velocity u_τ, and the thermal flux on the wall q_w; $y^+ = \dfrac{\rho u_\tau d}{\mu}$ is the dimensionless distance to the wall, where d is the shortest distance to the wall, and μ is the dynamic viscosity. The quantity T^+ is used to compute the thermal flux on the wall in the form (see [12])

$$T^+ = \frac{T_w - T_i}{T_\tau} = \frac{(T_w - T_i)\rho C_P u_\tau}{q_w} \Rightarrow q_w = \frac{(T_w - T_i)\rho C_P u_\tau}{T^+},$$

where $T_\tau = q_w/(\rho C_P u_\tau)$ is the friction temperature.

Next, we consider the most popular thermal wall functions.

One such function defined in [12] (it is denoted as **function A** below) is

$$T^+(y^+) = y^+ \,\mathrm{Pr}\, e^{(-\Gamma)} + \left\{2.12\ln\left[(1+y^+)\frac{2.5\left(2-\dfrac{y}{\delta}\right)}{1+4\left(1-\dfrac{y}{\delta}\right)^2}\right] + \beta(\mathrm{Pr})\right\} e^{(-1/\Gamma)},$$

where $\beta(\mathrm{Pr}) = (3.85\,\mathrm{Pr}^{1/3} - 1.3)^2 + 2.12\ln(\mathrm{Pr})$ and $\Gamma = 0.01\,(y^+\,\mathrm{Pr})^4/(1 + 5\,y^+\,\mathrm{Pr}^3)$.

This function is characterized by the presence of interpolation coefficients $e^{(-\Gamma)}$ and $e^{(-1/\Gamma)}$, which are used for the smooth switching between dependences for the laminar and logarithmic sublayers.

For flows with the Prandtl number $\mathrm{Pr} = 0.7$–1, the following wall function was proposed in [14] (it is denoted as **function B** below):

$$T^+(y^+) = \begin{cases} y^+\,\mathrm{Pr}, & y^+ \le 13.2, \\ 2.075\ln(y^+) + 13.2\,\mathrm{Pr} - 5.34, & y^+ > 13.2. \end{cases}$$

This function differs from function A by the dependence $T^+(y^+)$ in the logarithmic part of the boundary layer. In this function, the intersection point of the wall functions for the laminar and logarithmic sublayer is distinguished; at this point, there is a kink (see Fig. 1), which can result in poor iterative convergence and nonmonotonicity of the results as the grid is refined.

In [13], a function that includes a special formula for the more accurate definition of the distribution $T^+(y^+)$ in the transient sublayer (it is denoted as **function C** below) is proposed. It is defined by

$$T^+(y^+) = \begin{cases} y^+\,\mathrm{Pr}, & y^+\,\mathrm{Pr} < 1, \\ 1.87\ln(y^+\,\mathrm{Pr}+1) + 0.065y^+\,\mathrm{Pr} - 0.36, & 1 \le y^+\,\mathrm{Pr} \le 11.7, \\ 2.5\ln(y^+\,\mathrm{Pr}) - 1, & y^+\,\mathrm{Pr} > 11.7. \end{cases}$$

This function does not have considerable kinks in the profile $T^+(y^+)$ (see Fig. 1). Function C underestimates T^+ compared with functions A and B. This implies that function C gives a greater thermal flux in the boundary layer compared with functions A and B (Fig. 1).

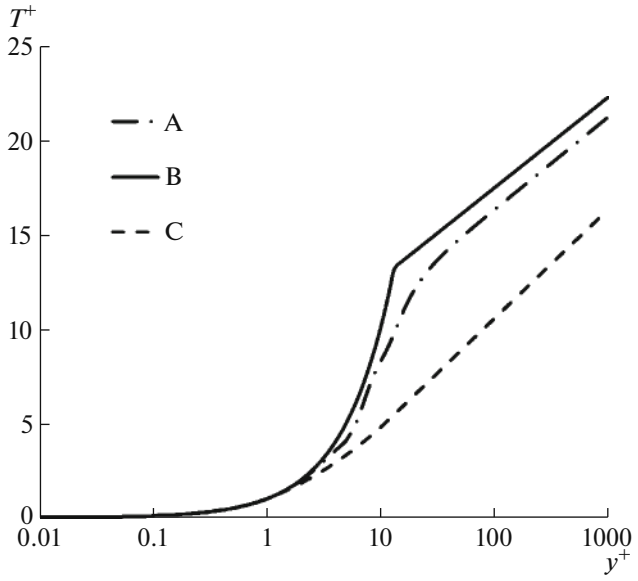

Fig. 1. Plot of dependence $T^+(y^+)$ for the wall functions A, B, and C.

Below, we present the results of comparing these wall functions applied to the simulation of forced convection with a thermal boundary layer. As the wall functions for friction on the wall, we use the universal wall functions (see [18])

$$U^+ = \frac{1}{\sqrt[4]{\dfrac{1}{U_{\text{vis}}^4} + \dfrac{1}{U_{\log}^4}}}, \quad U_{\text{vis}} = y^+, \quad U_{\log} = \frac{1}{\kappa}\log(Ey^+),$$

where $E = 7.3$ and $\kappa = 0.41$ is the Karman constant. The value U^+ is used for computing the friction τ_w:

$$u_\tau = U_1/U^+, \quad \tau_w = \rho u_\tau^2.$$

The turbulence kinetic energy k and the dissipation velocity of the turbulent energy ω in the near boundary cells are approximated by the expressions

$$k_1 = \left(\frac{1}{k_{\text{vis}}} + \frac{1}{k_{\log}}\right)^{-1}, \quad k_{\text{vis}} = 0.002u_\tau^2(y^+)^{3.5}, \quad k_{\log} = \frac{u_\tau^2}{0.3},$$

$$\omega_1 = \sqrt{(\alpha_{\text{vis}}\omega_{\text{vis}})^2 + \omega_{\log}}, \quad \omega_{\text{vis}} = \frac{80\nu}{d^2}, \quad \omega_{\log} = \frac{u_\tau}{0.3\kappa d},$$

where $\alpha_{\text{vis}} = 0.7$.

These formulas combine the approximation for the laminar (viscous) sublayer (vis) and for the logarithmic subregion (log). The expression making the largest contribution depends on the value of y^+ to which the boundary layer region corresponds.

The wall functions just described are used as boundary conditions for solving the system of hydrodynamic equations. For nonisothermal flows of viscous incompressible fluid, the Navier–Stokes system of equations supplemented by a turbulence model is used [16]. The numerical solution of such a system is considered in many studies; a detailed description can be found in [19–22].

In this paper, we use the SST model for simulating turbulence [16]. We find the numerical solution to the Navier–Stokes system of equations using the method SIMPLE based on finite volume approximation. A detailed description of this method can be found in [16, 19, 20]. The computations were performed using the Russian-made software package LOGOS designed for solving complex 3D problems of convective heat and mass transfer and fluid dynamics on parallel computers [4, 5, 7, 21, 22].

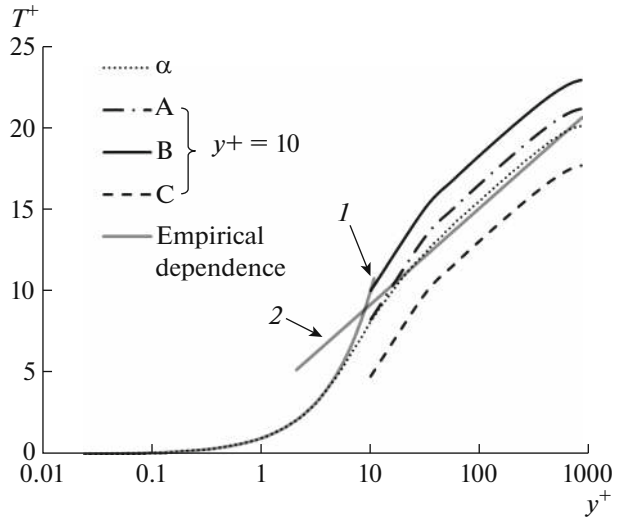

Fig. 2. Temperature profiles in the channel, α for the computation on the grid with $y^+ = 0.025$.

2. NUMERICAL EXPERIMENTS

We investigate the accuracy of simulating the turbulent boundary layer using the wall functions by solving the following problems concerning turbulent flow with heat exchange: flow in a plane channel [15], flow in a cannel with a moving wall (Couette's flow) [16], and flow around a flat plate [17]. The steady flow in a channel and Couette's flow are simple equilibrium flows that can be equally well computed on fine and on coarse grids. The problem of turbulent homogeneous flow around a plate is widely used for validating and verifying methodologies in computational fluid dynamics and turbulence models. The numerical computations were made for the Prandtl number $\mathrm{Pr} = 1$.

2.1. Flow in a Channel

We considered the problem of turbulent flow of incompressible fluid in a plane channel with cooled walls. The problem was solved for the Reynolds number $\mathrm{Re}_\tau = 900$ obtained based on the half height of the channel and the dynamic velocity u_τ on the wall. The temperature of the channel walls is constant $T = 0$. The volumetric energy release

$$Q = \frac{2\rho C_P}{\mathrm{Re}_\tau \mathrm{Pr}}$$

is specified in the computation domain. The flow of fluid is initiated by the source in the equation of momenta:

$$I_x = \frac{2\rho u_\tau^2}{h}.$$

Periodic boundary conditions are set on the input and output boundaries.

This problem was solved on different computational grids corresponding to different values of y^+. On the finest grid, y^+ corresponded to 0.025, and on the coarsest grid it was $y^+ = 60$. Each computational grid was refined near the walls, and the size of grid cells in the refined region varied at the rate of a geometric progression with the quotient 1.15.

In the steady flow, all the heat generated by the volumetric source leaves the domain through the thermal flux on the walls. The unknown quantity in this problem is the distribution of temperature and its maximum value, which is achieved in the center of the channel. If the thermal flux q_w is underestimated, then the maximum temperature $T^+_{\max}$ is overestimated; conversely, if the thermal flux is overestimated, then the maximum temperature is underestimated.

Figure 2 shows the profiles of the dimensionless temperatures T^+ on the grids with $y^+ = 10$ obtained using the thermal functions under consideration.

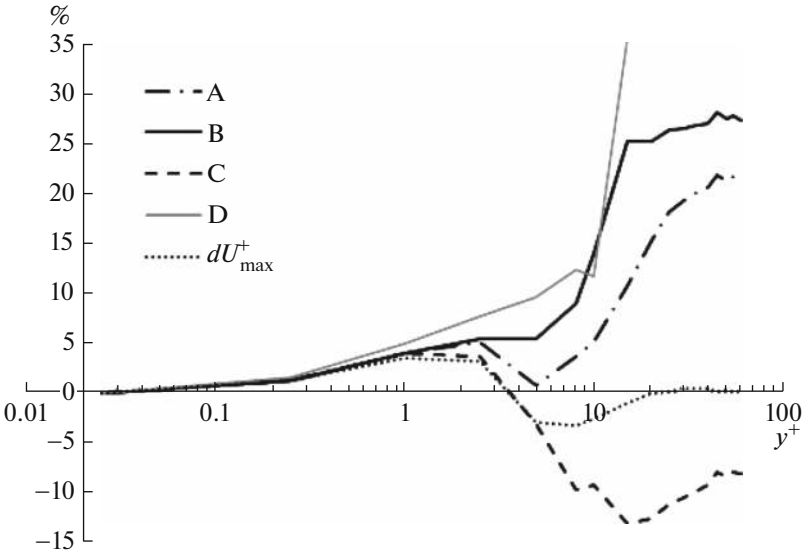

Fig. 3. Deviation of the maximum temperature and maximum velocity as a function of y^+.

The temperature profile obtained on the finest grid with $y^+ = 0.025$ is in good agreement with the empirical dependence [23] represented by the formulas $T^+ = y^+$ and $T^+ = 5.91\lg(y^+) + 3.26$, which are illustrated in Fig. 2 by curves 1 and 2. The result with the lowest y^+ is independent of the choice of the wall function because the boundary layer is numerically resolved up to the laminar sublayer in which the heat transfer is mainly caused by heat conduction. As y^+ increases, different wall functions give deviations from the empirical profile. For the analysis of results, it is convenient to consider the deviation

$$dT^+_{\max} = \frac{T^+_{\max} - T^0_{\max}}{T^0_{\max}},$$

where $T^0_{\max}$ is the maximum dimensionless temperature obtained on the finest grid $y^+ = 0.025$.

Figure 3 illustrates the deviations of the maximum temperature and the maximum velocity as functions of y^+: the curves A, B, and C represent the deviation of the maximum temperature obtained for the functions A, B, and C, respectively; the curve D represents the deviation of the maximum temperature obtained without using the wall function; and the curve $dU^+_{\max}$ represents the deviation of the maximum velocity

$$\frac{U^+_{\max} - U^0_{\max}}{U^0_{\max}},$$

where $U^0_{\max}$ is the maximum dimensionless velocity obtained on the finest grid.

It is seen in Fig. 3 that up to $y^+ = 1$ the wall function give approximately the same deviation, which coincides with the maximum velocity deviation in the channel center. This indicates that the error in the work of the thermal wall functions is probably caused by the error in the work of the friction wall function. Beyond $y^+ = 1$, there variations are of different nature. As could be expected, the error in the solution obtained without using the wall functions quickly increases when $y^+ > 10$. The maximum error for the functions A, B, and C is 20%, 28%, and 13%, respectively. However, the function B gives a steadily increasing error, while the two other functions demonstrate a nonmonotonic behavior of the result. For example, for the functions A and B, in the domains $y^+ \approx 5$ and $y^+ \approx 3$, respectively, the deviation is lower than on finer grids with lower y^+. In practice, this can deteriorate the simulation results as the computation grid is refined.

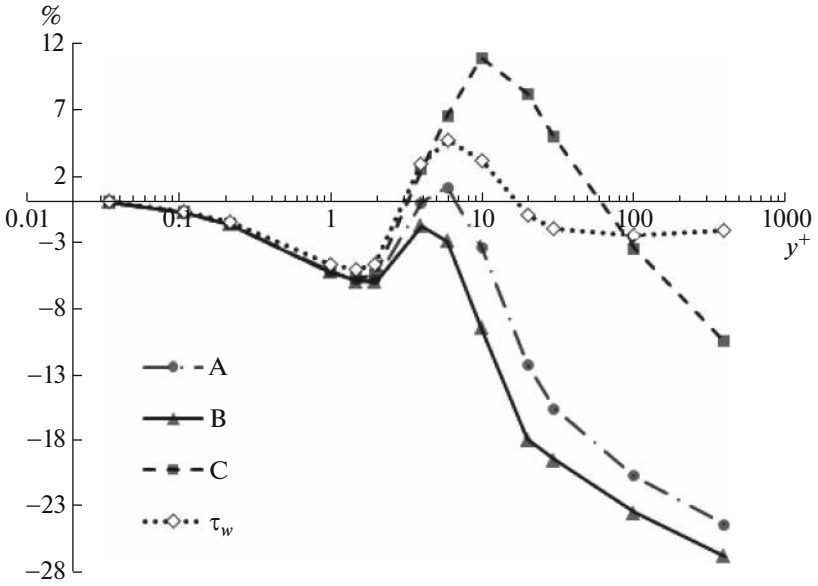

Fig. 4. Deviation of the thermal flux and friction stress on the wall as a function of y^+.

2.2. Channel with a Moving Wall

In this subsection, we consider the steady turbulent flow of incompressible fluid in a plane channel with a moving heated wall (Couette's flow). The problem was solved with the Reynolds number $\mathrm{Re} = u_w h/\nu = 10^6$, where u_w is the wall velocity and h is the channel height. The temperature on the moving wall is constant, $T = 1$, and the temperature on the stationary wall is also constant, $T = 0$. Periodic boundary conditions are specified on the input and output boundaries of the channel. The problem was solved on different grids with $y^+ = 0.035$ for the finest grid and $y^+ = 400$ for the coarsest grid. The grid was refined at the rate of a geometric progression with the quotient 1.15.

After the flow steadies, the temperature profile becomes centrally symmetric about the channel center, and the thermal flux q_w on the moving and stationary walls becomes equal. Figure 4 shows the deviation of the thermal flux on the wall from the solution obtained on the finest grid with $y^+ = 0.035$.

It is seen from these plots that, as in the preceding problem, the deviations of the thermal flux for $y^+ \le 2$ are similar to the deviations of the friction coefficient. The function C gave the worst result on the grids with $y^+ > 6$, where the error was as high as almost 26%. The function A gave the error of 24% for $y^+ > 10$; however, in the interval $2 < y^+ < 10$ it gave better results than the function A. The function C demonstrated a high error for $2 < y^+ < 30$, which reached 11%. All the functions demonstrated a nonmonotonic behavior of the result as the grid is refined.

2.3. Flow around a Plate

In this subsection, we consider the two-dimensional homogeneous turbulent flow around a heated flat plate. The problem was solved with the Reynolds number $\mathrm{Re} = u_\infty L/\nu = 10^7$ at the end of the plate, where u_∞ is the velocity of the incident flow and $L = 1$ is the plate length. Figure 5 shows an example of the computation grid for this problem. The height of the computation domain is $h = 0.25$. On the boundary AB, the incoming flow with the fixed velocity u_∞ and temperature $T = 0$ is specified. The boundary CD is the plate surface with the fixed temperature $T = 1$. The boundary BC is a segment of length $0.03L$ ahead of the plate. Symmetric boundary conditions are specified on the boundaries BC and AE. The boundary condition with the zero static pressure is specified on the boundary ED. The problem was solved on different grids corresponding to the parameter $y^+ = 0.18$–180 on the trailing edge of the plate. The height of the grid cells increased at the rate of a geometric progression with the quotient 1.15 with recede from the plate surface. The number of grid cells along the direction x was the same for all grids, and their width increased at the rate of a geometric progression with the quotient 1.15; the minimal grid step was 0.0005, and the maximal size was 0.04.

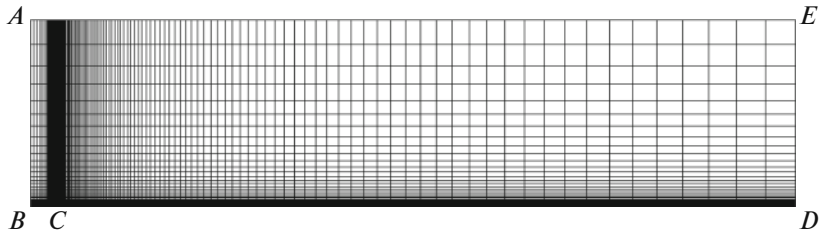

Fig. 5. Example of the computation grid for the plate flow problem.

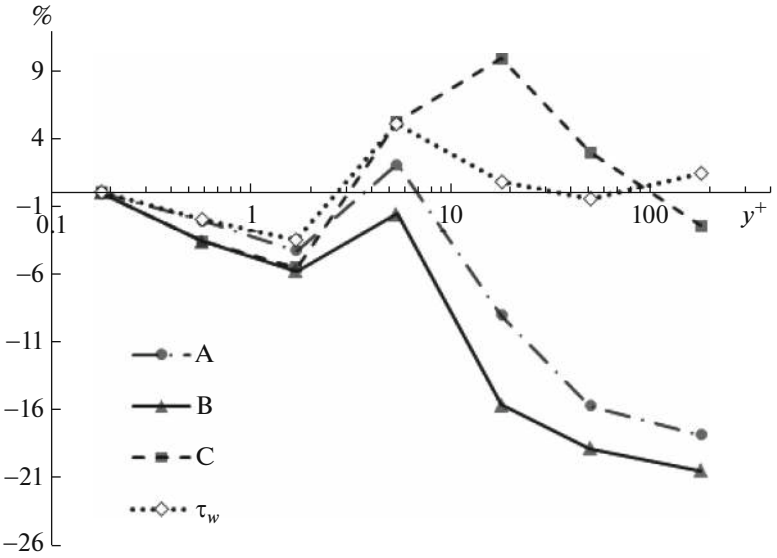

Fig. 6. Deviation of the thermal flux and friction stress on the wall from the limiting solution.

After the flow becomes steady, the tangent friction stress on the plate and the thermal flux decrease when receding from the plate's leading edge. The thermal flux was measured on the plate at the point at the distance x from the plate's leading edge; this distance corresponds to the local Reynolds number $\mathrm{Re}_x = xu_\infty/\nu \approx 8.7 \times 10^6$. Figure 6 shows the plot of thermal fluxes q_w on grids with different y^+.

The results in Fig. 6 are similar to the results obtained for the preceding problem. The function C demonstrates the nonmonotonicity of results and a high deviation at the medium values of y^+. The function A demonstrates a high deviation up to 18% on coarse grids. For the function B, the deviation is the highest reaching as high as 20%.

The solution of three problems using three wall thermal functions showed that none of the examined approximations gives the minimally acceptable error. The wall function A provides better results for $y^+ < 10$; however, the deviation of the thermal characteristics grows on coarse grids. The function B provides large deviations in the logarithmic sublayer, in which it tends to overestimate T^+. The function C gives the highest deviation of results in the interval $1 \le y^+ \mathrm{Pr} \le 11.7$. Another drawback of the functions considered above is the nonmonotonic convergence of the results as the computation grid is refined.

CONCLUSIONS

The accuracy of simulating the thermal boundary layer on grids with different resolutions in the boundary layer and with different thermal wall functions described in [12–14] was examined. These wall functions were used to perform a series of computations of the turbulent nonisothermal flow of fluid in channels and along a plate with the Prandtl number $\mathrm{Pr} = 1$.

It was found that the use of the function [13] gives the lowest error in the estimation of the dimensionless temperature on coarse grids compared with the other functions. However, this function gives a large deviation in the intermediate domain. The functions described in [12, 14] give the deviation that grows up to 20% with increasing y^+. The study also showed that all the examined function can give a nonmonotonic convergence when the computation grid is refined. In practice, this can deteriorate the simulation results as the computation grid is refined.

FUNDING

The results of were obtained within the state research program, project nos. 5.4568.2017/6.7 and 5.1246.2017/4.6. The work was also supported by the Presidential program of Support of Leading Scientific Schools, project no. NSh-2685.2018.5; by the Presidential program of support of young Russian doctors of science, project no. MD-4874.2018.9; and by the Russian Foundation for Basic Research, project no. 16-01-00267.

REFERENCES

1. H. Schlichting, *Boundary Layer Theory,* 6th ed. (McGraw-Hill, New York, 1968).
2. A. Yu. Snegirev, *High-Performance Computations in Physics: Numerical Simulation of Turbulent Flows* (Politekhnicheskii Univ., St. Petersburg, 2009) [in Russian].
3. P. R. Spalart, "Strategies for turbulence modeling and simulations," Heat Fluid Flow **21**, 252–263 (2000).
4. A. S. Kozelkov, O. L. Krutyakova, V. V. Kurulin, S. V. Lashkin, and E. S. Tyatyushkina, "Application of numerical schemes with singling out the boundary layer for the computation of turbulent flows using eddy-resolving approaches on unstructured grids," Comput. Math. Mat. Phys. **57**, 1036–1047 (2017).
5. A. S. Kozelkov, V. V. Kurulin, S. V. Lashkin, R. M. Shagaliev, and A. V. Yalozo, "Investigation of supercomputer capabilities for the scalable numerical simulation of computational fluid dynamics problems in industrial applications," Comput. Math. Mat. Phys. **56**, 1506–1516 (2016).
6. I. A. Belov and S. A. Isaev, *Simulation of Turbulent Flows: A Texbook* (Baltic State Technical Univ. St. Petersburg, 2001) [in Russian].
7. A. S. Kozelkov, Yu. N. Deryugin, Yu. A. Tsibereva, A. V. Kornev, O. V. Denisova, D. Yu. Strelets, A. A. Kurkin, V. V. Kurulin, I. L. Sharipova, D. P. Rubtsova, M. A. Legchanov, E. S. Tyatyushkina, S. V. Lashkin, A. V. Yalozo, S. V. Yatsevich, N. V. Tarasova, R. R. Ginniyatullin, M. A. Sizova, and O. L. Krutyakova, "The minimal set of benchmarks for validating methods of numerical simulation of turbulent lows of viscous incompressible fluid," Trudy Nizh. Gos. Tech. Univ., No. 4 (106), 21–69 (2014).
8. B. E. Launder and D. B. Spalding, "The numerical computation of turbulent flows," Comput. Meth. Appl. Mech. Eng. **3**, 269–289 (1974).
9. A. S. Kozelkov, V. V. Kurulin, O. L. Puchkova, and S. V. Lashkin, "Simulation of turbulent flows using the algebraic Reynolds stress model with universal near-wall functions," Vychisl. Mekh. Sploshnykh Sred **7** (1), 40–51 (2014).
10. L. I. Zaichik, "Wall functions for simulation of turbulent flows and heat transfer, High. Temp. **35**, 385–390 (1997).
11. S. A. Isaev, P. A. Baranov, A. G. Sudakov, and I. A. Popov, "Verification of the standard model of shear stress transport and its modified version that takes into account the streamline curvature and estimation of the applicability of the Menter combined boundary conditions in calculating the ultralow profile drag for an optimally configured cylinder–coaxial disk arrangement," Tech. Phys. **61**, 1151–1161 (2016).
12. B. A. Kader, "Temperature and concentration profiles in fully turbulent boundary layers," Int. J. Heat Mass Transfer **24**, 1541–1544 (1981).
13. P. L. Kirillov, Yu. S. Yur'ev, and V. P. Bobkov, *Handbook of Heat and Hydraulic Computations (Nuclear Reactors, Heat Exchangers, and Steam Generators)* (Energoatomizdat, Moscow, 1990) [in Russian].
14. W. M. Kays and M.E. Crawford, *Convective Heat and Mass Transfer* (McGraw-Hill, New York, 1994).
15. J. Kim and P. Moin, *Transport of Passive Scalars in a Turbulent Channel Flow*, Vol. VI (Springer, Berlin, 1989).
16. F. R. Menter, M. Kuntz, and R. Langtry, "Ten years of experience with the SST turbulent model," Turbulence, Heat and Mass Transfer 4, ed. by K. Hanjalic, Y. Nagano, and M. Tummers (Begell House Inc, 2003).
17. K. Wieghardt and W. Tillmann, "On the turbulent friction layer for rising pressure," NACA TM-1314 (1951).
18. E. M. Smirnov and D. K. Zaitsev, "Modification of wall boundary conditions for low-Re k-w turbulence models aimed at grid sensitivity reduction," *Proc. of the Europ. Conf. for Aerospace Sci., Moscow, 2005* (EUCASS 2005), ID 2.09.06.
19. J. H. Ferziger and M. Peric, *Computational Methods for Fluid Dynamics* (Springer, Berlin, 2001).
20. A. S. Kozelkov, "Implementation of a method for the computation of viscous incompressible fluid using the multigrid method and the SIMPLE algorithm in the software package LOGOS," Voprosy Atom. Nauki Tekhn., Ser. Math. Model. Phys. Proc. No. 4 (2013).
21. K. N. Volkov, A. S. Kozelkov, S. V. Lashkin, N. V. Tarasova and A. V. Yalozo, "A parallel implementation of the algebraic multigrid method for solving problems in dynamics of viscous incompressible fluid," Comput. Math. Mat. Phys. **57**, 2030–2046 (2017).
22. A. S. Kozelkov, A. A. Kurkin, V. V. Kurulin, M. A. Legchanov, E. S. Tyatyushkina, and Yu. A. Tsibereva, "Investigation of the application of RANS turbulence models to the calculation of nonisothermal low-Prandtl-number flows," Fluid Dyn. **50**, 501–513 (2015).
23. E. U. Repik and Yu. P. Sosedko, *Turbulent Boundary Layer: Methodology and Experimental Results* (Fizmatlit, Moscow, 2007) [in Russian].

Translated by A. Klimontovich